Soft Matter

Oblique Interface Shearing (OIS): Single-step Microdroplet Generation and On-Demand Positioning

Journal:	*Soft Matter*
Manuscript ID	SM-COM-02-2019-000263.R1
Article Type:	Communication
Date Submitted by the Author:	30-Mar-2019
Complete List of Authors:	Huang, Fangsheng; University of Science and Technology of China, Hefei; Ohio State University Niu, Ye; The Ohio State University, Department of Biomedical Engineering; The Ohio State University, Department of Mechanical and Aerospace Engineering Zhu, Zhiqiang; University of Science and Technology of China, Huang, Hanyang; The Ohio State University Xue, Yue; University of Science and Technology of China; Ohio State University Si, Ting; University of Science and Technology of China, Department of Modern Mechanics; The Ohio State University, Department of Biomedical Engineering Xu, Ronald; University of Science and Technology of China, Hefei; The Ohio State University Zhao, Yi; The Ohio State University,

Oblique Interface Shearing (OIS):

Single-step Microdroplet Generation and On-Demand Positioning

Fangsheng Huang[1, 2, a)], Ye Niu[2, 3, a)], Zhiqiang Zhu[1], Hanyang Huang[2], Yue Xue[1, 2], Ting Si[4], Ronald X. Xu[1, 2, b)], and Yi Zhao[2, 3, b)]

[1]Department of Precision Machinery and Precision Instrumentation, University of Science and Technology of China, Hefei, Anhui 230026, People's Republic of China

[2]Department of Biomedical Engineering, The Ohio State University, Columbus, Ohio 43210, USA

[3]Department of Mechanical and Aerospace Engineering, The Ohio State University, Columbus, Ohio 43210, USA

[4]Department of Modern Mechanics, University of Science and Technology of China, Hefei, Anhui 230026, People's Republic of China

[a)] F. Huang and Y. Niu contributed equally to this work.

[b)] Authors to whom all correspondences should be addressed:

xu.202@osu.edu and zhao.178@osu.edu

Abstract:

A new process for simultaneous generation and positioning of microdroplets within a single step named oblique interface shearing (OIS) is reported based on the observation that liquid microdroplets generated by vibrating a thin capillary across the air-liquid interface at an oblique angle exhibit notable lateral displacements. An analytical model is established to describe the lateral droplet displacement induced by the Stokes drift effect. The dependency of the lateral displacement on typical operating parameters allows for on-demand droplet positioning while they are produced. The efficacy of the process is validated through delivering microdroplets with the same size to different positions as well as size-dependent positioning of these microdroplets.

Cross-interface emulsification is a new process recently reported to generate monodisperse microdroplets by vibrating a thin capillary across an air-liquid interface.[1-4] Different from the atomization processes based on Plateau-Rayleigh instability (such as electrospray and flow focusing) where the droplet volume is vulnerable to the changes of many operating parameters as well as the environmental conditions, the droplet volume by cross-interface emulsification depends solely on the flow rate and the vibration frequency of the capillary.[1, 2] The excellent droplet size uniformity, good process controllability, and simple configuration make it a promising fabrication approach of generating microdroplets for various biomedical applications.[5, 6] In this process, the capillary vibrates across the air-liquid interface vertically. The as-formed microdroplets align themselves in a vertical stream and slowly sediment to the bottom of the container (Fig. 1(a)). Although microdroplets of different sizes can be made by tuning the flow rate and the vibration frequency, extra efforts is needed to deliver the microdroplets of different sizes to desired positions for future uses.[7-11]

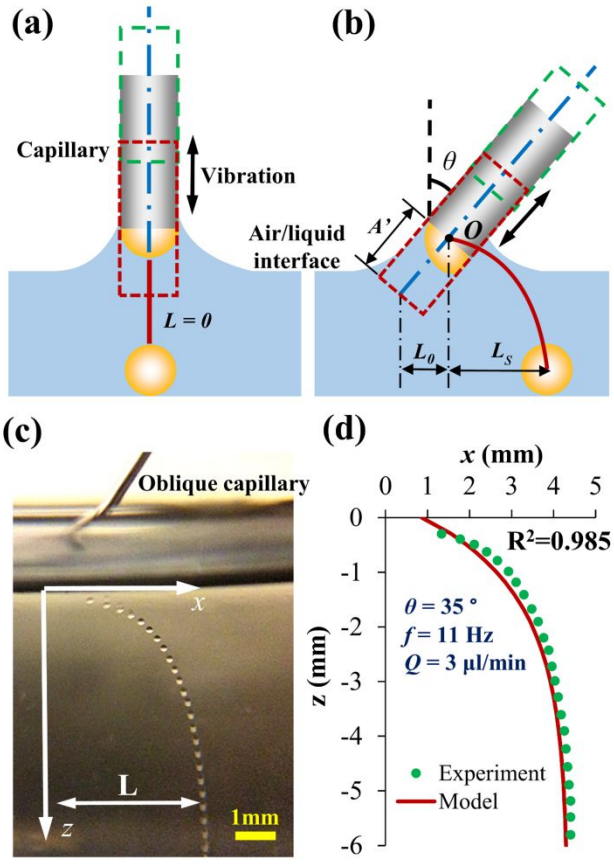

FIG. 1. Schematics of cross-interface emulsification and oblique interface shearing (OIS). (a) Schematic of cross-interface emulsification. (b) Schematic of the OIS process. (c) A typical microdroplet trajectory in OIS. (d) The comparison of experimentally measured trajectory (green dots) with the model prediction (solid red curve).

In this letter, we propose an oblique interface shearing (OIS) process where the capillary vibrates across the air-liquid interface at an oblique angle θ (*i.e.,* not equals 90°). The microdroplets generated by OIS are observed to move laterally as they sediment to the bottom of the container. The relation of the ultimate lateral displacement with the oblique angle, the vibration frequency of the capillary and the flow rate of the dispersed phase are investigated to explore the possibility of positioning the microdroplets to desired locations as they are produced.

Different from previously reported cross-interface emulsification where the microdroplets sediment vertically, the microdroplet in OIS exhibits a lateral displacement after leaving the capillary tip. The lateral displacement is denoted by L_s with the lateral position of the droplet when it leaves the capillary tip (denoted as *O* in Fig. 1(b)) as the reference. Due to the technical difficulty of measuring the exact position of *O*, the lowest position of the vibrating capillary tip is used as the reference. The lateral droplet displacement can thus be expressed as $L = L_s + L_0$, where $L_0 = A' \sin\theta$, A' is the maximal immersing length of the capillary, and θ is the oblique angle. The periodic tapping motion of the capillary tip across the air-liquid interface generates a series of single capillary waves. The position of the tip was adjusted to have the tip quickly re-submerged into the liquid after the last withdrawing action. In other words, the airborne time of the tip is very short. The series of the single waves can thus be approximated as a continuous wave.[12] The horizontal droplet motion can be estimated using the Stokes drift mean velocity equation: [13]

$$\frac{dx}{dt} = \frac{-4\pi^2 a^2}{\lambda T} e^{-4\pi z(t)/\lambda} \quad (1),$$

where x and z are the lateral and vertical droplet displacements; and a, λ, and T are the amplitude, wavelength, and period of the waves, respectively. The vertical droplet motion is governed by:

$$G - F_b - F_{drag,\ z} = m\frac{d^2 z}{dt^2} \quad (2),$$

where $G = \rho_0 g V$ is the gravitational force of the droplet; $F_b = \rho_m g V$ is the buoyancy force; $F_{drag,\ z} = 3\pi\eta(dz/dt)D$ is the vertical drag force; m, V, and D are the mass, volume, and

diameter of the droplet, ρ_0 and ρ_m are the densities of the droplet and of the medium in the container, respectively; and η is the dynamic viscosity of the medium in the container. The trajectories of the as-formed microdroplets can be derived from *Eqns. (1)* and *(2)*. The results show that the vertical velocity of the microdroplet increases gradually and eventually reaches a plateau when the gravitational force reaches the equilibrium with the drag force and buoyancy force. The mean lateral velocity decreases as the microdroplet sediments (Fig. 1(c) and Video 1 in supplementary materials). Such prediction has a good agreement with the experimental observation (Fig.1(d)), with the coefficient of correlation of $R^2>0.985$. With a deep enough collecting container, the ultimate L_s has the form of:

$$L_s|_{t=\infty} = \frac{18\pi\eta a^2 f}{(\rho_0 - \rho_m)gD^2} \quad (3).$$

Similar as in previous cross-interface emulsification, the droplet diameter in the OSI process (D) is solely determined by the flow rate Q and the vibration frequency f of the capillary as:[1-3]

$$D = \sqrt[3]{3Q/\pi f} \quad (4).$$

The wave amplitude positively relates to the capillary force at the air-liquid interface. With a given capillary caliber, a large capillary force can lead to a large wave amplitude. In OIS, the capillary force increases with the oblique angle as expresses as $F_{\text{capillary}} = \pi D\gamma/cos\theta$, where γ is the surface tension.[14] By assuming the wave amplitude changes linearly with the capillary force, the amplitude of the OIS induced wave can be estimated as $a_0/cos\theta$, where a_0 is the amplitude of the wave induced by a vertical capillary. The ultimate lateral displacement can be expressed as:

$$L|_{t=\infty} = L_s|_{t=\infty} + L_0 = \frac{12\pi\eta(a_0/\cos\theta)^2}{(\rho_0-\rho_m)g} f^{5/3} Q^{-2/3} + A'\sin\theta \quad (5).$$

It should be noted that at $\theta = 0^o$, the microdroplets are generated at the standing point of the waves and not subject to the effect of the Stokes drift. In this case, *Eqn. (2)* should be used to describe the trajectory of droplets.

Eqn. (5) shows that in OIS the ultimate lateral displacement $L|_{t=\infty}$ is not only a function of the oblique angle, but also varies with the vibration frequency, and the flow rate. In particular, $L|_{t=\infty}$ increases with the increasing oblique angle. At a given oblique angle, $L|_{t=\infty}$ can be increased by increasing the vibration frequency or decreasing the flow rate. However, changing these operating parameters may affect the process stability. This was experimentally investigated. A metallic capillary with the inner diameter of 260 μm and the outer diameter of 460 μm was mounted at an oblique angle, which was driven by a vibrator and controlled by a function generator. Photocurable ethoxylated trimethylolpropane triacrylate (ETPTA) resin (the disperse phase) was pumped through the capillary and dispersed into an aqueous solution with 0.5 *wt%* polyvinyl alcohol and 0.5 *wt%* sodium lauryl sulfate (the continuous phase) using a syringe pump. The free surface of the aqueous solution is about 20 *mm* to the container bottom. The relation between the process stability and the operating parameters (the oblique angle θ, the vibration frequency f, and the flow rate Q) is shown in Fig. 2(a), where blue dots represent the conditions that can form microdroplets in a stable manner; and red dots represent the conditions of unsuccessful or unstable droplet formation. The experimental results show that the process

instability tends to occur at low flow rates, high vibration frequencies, and large oblique angles. As shown in Fig. 1(c), droplets are formed by shearing the disperse phase off the capillary tip. At a very low flow rate, the meniscus curvature at the interface between the disperse phase and the continuous phase is too small to allow the disperse phase be sheared off the capillary tip in a repeatable pattern. The unstable droplet generation at high vibration frequency may be due to the frequency mismatch between the capillary tip vibration and the induced surface waves. The unstable droplet generation at a large oblique angle is primary due to the limited vibration amplitude, *i.e.,* the capillary tip cannot always vibrate across the air-liquid interface at a very large oblique angle. The window of operating parameters that allow stable droplet generation was determined. In particular, at θ=35°, stable droplet generation can be achieved with f ranges from 3 *Hz* to 12 *Hz*, and Q ranges from 1 $\mu l/min$ to 5 $\mu l/min$ (Fig. 2(b)). Within this window, the ultimate lateral displacement $L|_{t=\infty}$ increases linearly with $f^{5/3}$ (Fig. 2(c) and Video 2 in supplementary materials), and increases linearly with $Q^{-2/3}$ (Fig. 2(d) and Video 3 in supplementary materials), similar as predicted by *Eqn. (5)*, except for a few unstable conditions.

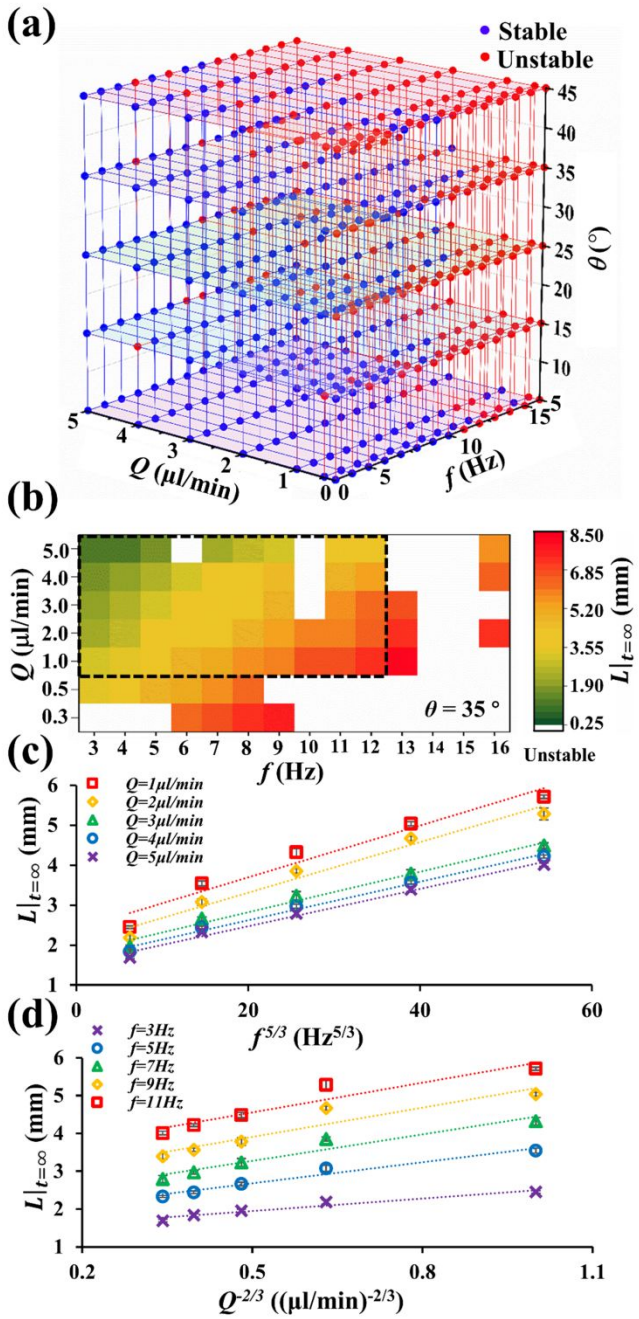

FIG. 2. The process stability and the influence of operating parameters on the lateral displacement. (a) The window of stable microdroplet generation, where blue dots denote stable conditions, and red dots denote unstable conditions. (b) Contour maps of experimentally measured process stability and ultimate lateral displacement under the oblique angle of 35°. (c&d) The change of ultimate lateral displacement with (c) the vibration frequency and (d) the flow rate at the oblique angle of 35º. The dashed lines in (c) denote the linear fittings with constant $\frac{d(L|_{t=\infty})}{d(f^{5/3})}$ values; and the dashed lines in (d) denote the linear fittings with constant $\frac{d(L|_{t=\infty})}{d(Q^{-2/3})}$ values.

OIS allows for the precise delivery of microdroplets of desired sizes to different lateral positions. According to *Eqn. (4)*, the droplet size solely depends on the ratio between the flow rate and the vibration frequency (*Q/f*). It is thus possible to change $L|_{t=\infty}$ by either changing the oblique angle (Fig. 3(a)), the vibration frequency (Fig. 3(b)), the flow rate, or their combinations while keeping a constant *Q/f*. Here, we kept the *Q/f* =1/3 ($\mu l \cdot min^{-1}/Hz$). The measurement shows that the ultimate lateral displacement increases from 1.59 *mm* at 3 *Hz* to 3.63 *mm* at 15 *Hz*. The average size of microdroplets exhibits a very small variation (around 219 μm to 222 μm) from the value predicted by *Eqn. (4)* (220 μm) within the frequency range from 6 *Hz* to 15 *Hz*. However, a relatively large size deviation was seen under 3*Hz*, where the average size was measured as 238 μm. This is probably due to the reduced accuracy of the linear motor in the syringe pump when it operates at the speed close to the lower limit.

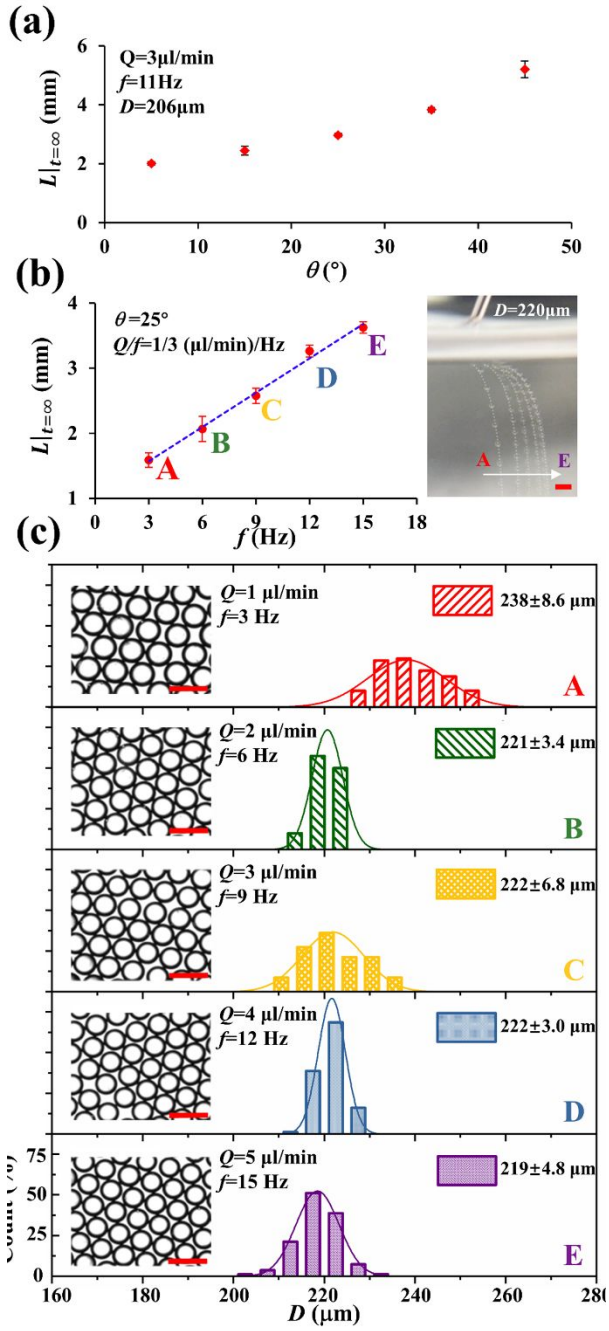

FIG. 3. Generation and positioning of microdroplets of the same size to desired locations. (a) The change of the ultimate lateral displacement with the oblique angle θ under given Q and f; (b) The ultimate lateral displacement changes linearly with the vibration frequency f at a constant Q/f value of 1/3 $(\mu l \cdot min^{-1}/Hz)$. The inset shows the overlapped images. Scale bar: 500 μm; and (c) The size distribution of microdroplets delivered to different lateral positions. n = 100 for each group.

Another unique beauty of the OIS process is to displace microdroplets of different sizes as they are produced. This was demonstrated by placing a laser engraved multi-compartment collector in the continuous phase. The collector consists of three rectangular compartments with a linear arrangement. The adjacent compartments are separated by a thin wall that is 250 μm wide and 1mm high. The collector was positioned to have one compartment (Compartment 1) sit underneath the intersection between the liquid surface and the oblique capillary ($\theta = 35°$), while the other two compartments have lateral displacements to the intersection point. Here, the flow rate was kept as 2 $\mu l/min$. At the frequency of 3 Hz, the droplets exhibited a small $L|_{t=\infty}$ and fell in the Compartment 1. As the frequency increased to 7 Hz, $L|_{t=\infty}$ increased and brought the following droplets in the adjacent compartment (Compartment 2). The droplets started to enter Compartment 3 as the frequency increased to 12 Hz (Fig. 4(a-c)). The average size of the droplets in the three compartments are 277 μm in Compartment 1, 209 μm in Compartment 2, and 172 μm in Compartment 3, respectively. The average size decreases with increasing $L|_{t=\infty}$. The droplet size in each compartment shows a small standard derivation (Fig. 4(d)).

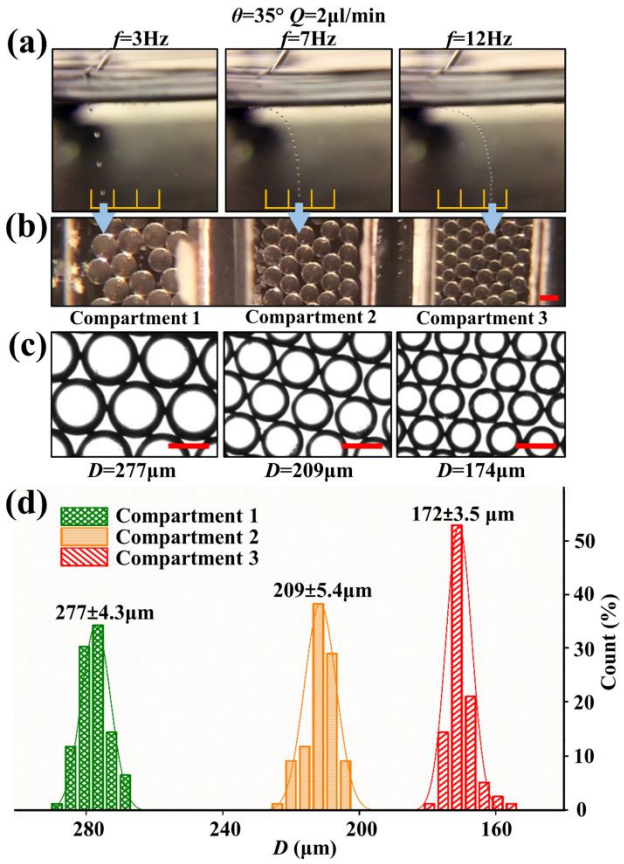

FIG. 4. Simultaneous generation and size dependent displacement of microdroplets by the OIS process. (a) The trajectories of droplets under different frequencies; (b-c) The microscopic images in different compartments; and (d) The size distribution in the three compartments. $Q = 2\ \mu l/min$ and $\theta = 35°$. ($n = 100$ for each group. Scale bar: 200 μm)

In summary, microdroplets formed by passing a vibrating oblique capillary through the air-liquid interface exhibit lateral displacement due to the Stokes drift induced by the vibrating motion. The lateral displacement of the microdroplets varies with the oblique angle, the vibration frequency, and the flow rate of dispersed phase through the capillary tip. In the OIS process developed upon this phenomenon, microdroplets of the same size can be produced and delivered to different lateral positions as needed. Microdroplets of different sizes can be produced and delivered to desired positions based on their sizes. Analytical

and experimental studies demonstrate the technical feasibility of simultaneous generation and positioning of microdroplets on demand for their future uses in various applications.

See supplementary material for videos of the OIS process: (**Video 1**): Microdroplet formation and the Stokes drift effect in the OIS process under the frame rate of 10,000 *fps*. (**Video 2**): The change of microdroplet trajectories under varied vibration frequencies (from 1 *Hz* to 12 *Hz*). The oblique angle is 35°, and the flow rate is 2 *μl/min*. (**Video 3**): The change of microdroplet trajectories under varied flow rates (from 1 *μl/min* to 5 *μl/min*). The oblique angle is 35°, and the vibration frequency is 12 *Hz*.

Acknowledgments

This work was supported by National Science Foundation through the grants 1509727 and 1701038 (Y.Z.), and National Natural Science Foundation of China (Nos. 11472270, 11722222, 81327803, and 11621202) (R.X.). The authors would like to thank the support of a facilities grant generously provided by Institute for Materials Research at OSU (Y.Z.).

References

1. S. Liao, Y. He, D. Wang, L. Dong, W. Du and Y. Wang, *Advanced Materials Technologies*, 2016, **1**, 1600021.
2. P. Xu, X. Zheng, Y. Tao and W. Du, *Analytical chemistry*, 2016, **88**, 3171-3177.
3. M. Valet, L.-L. Pontani, A. Prevost and E. Wandersman, *Physical Review Applied*, 2018, **9**, 014002.
4. S. Liao, Y. Tao, W. Du and Y. Wang, *Langmuir*, 2018, **34**, 11655-11666.
5. Y. Hu, P. Xu, J. Luo, H. He and W. Du, *Analytical chemistry*, 2016, **89**, 745-750.
6. S. Liao, X. Tao, Y. Ju, J. Feng, W. Du and Y. Wang, *ACS applied materials & interfaces*, 2017, **9**, 43545-43552.
7. D. Huh, J. H. Bahng, Y. Ling, H.-H. Wei, O. D. Kripfgans, J. B. Fowlkes, J. B. Grotberg and S. Takayama, *Analytical chemistry*, 2007, **79**, 1369-1376.
8. M. Chabert and J.-L. Viovy, *Proceedings of the National Academy of Sciences*, 2008, **105**, 3191-3196.
9. D. R. Gossett, W. M. Weaver, A. J. Mach, S. C. Hur, H. T. K. Tse, W. Lee, H. Amini and D. Di Carlo, *Analytical and bioanalytical chemistry*, 2010, **397**, 3249-3267.
10. P. Sajeesh and A. K. Sen, *Microfluidics and nanofluidics*, 2014, **17**, 1-52.
11. M. Li, M. van Zee, K. Goda and D. Di Carlo, *Lab on a Chip*, 2018, **18**, 2575-2582.
12. M. Bakhoday-Paskyabi, *Ocean Dynamics*, 2015, **65**, 1063-1078.
13. F. Mugele, A. Staicu, R. Bakker and D. van den Ende, *Lab on a Chip*, 2011, **11**.
14. C. Raufaste, G. Kirstetter, F. Celestini and S. Cox, *EPL (Europhysics Letters)*, 2012, **99**, 24001.

Shearing a continuous stream at the air/liquid interface with an oblique angle allows for generation and on-demand positioning of microdroplets

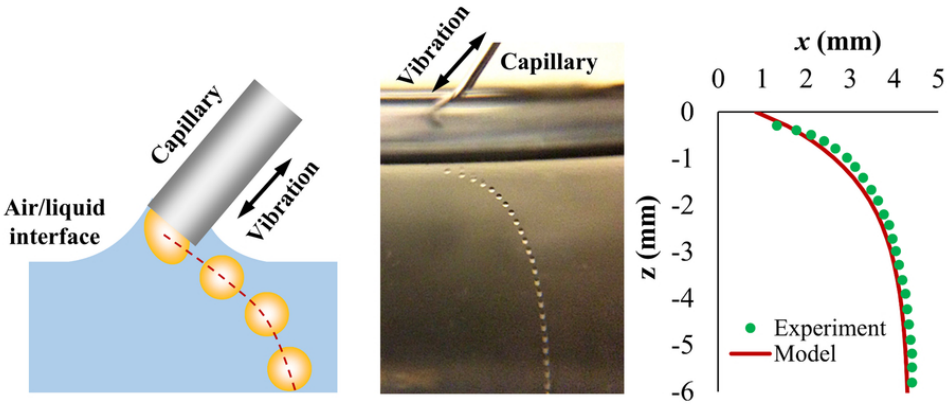

80x39mm (300 x 300 DPI)